Model Globally, Measure Locally!

Mauna Loa

A JAMSTEC-NOAA-IPRC collaboration explores the fine-scale structure of atmospheric thermal tidal oscillations.

The great 18th century German explorer and naturalist Alexander von Humboldt famously wrote that in the tropics the variation of atmospheric pressure through the day is so regular that a barometer can be used instead of a clock to tell the local time! As a randomly chosen example, Figure 1 shows the pressure at Hilo Airport on the Big Island of Hawai'i (19.7°N) for 48 hours in February 2008. Although over the full 48-hour period the pressure falls as the synoptic-scale weather pattern evolves, the pressure reaches a peak around 9–10 o'clock each morning and evening— a pattern repeated almost every day at all locations in the tropics.

This regular daily march of barometric pressure is a surface manifestation of the atmospheric thermal tides excited by the daily cycle of solar radiation. The atmospheric tides are global phenomena and an adequate theoretical treatment requires a global model. However, the tides are also modulated by local variations in topography, leading to an interesting dynamical problem involving interaction of very disparate scales of motion. Such multiscale problems are common in meteorology and are particularly difficult to investigate using observational diagnostic approaches, since appropriately detailed observations are typically not available globally at high resolution. The advent of comprehensive global atmospheric simulation models that can be run at very fine spatial resolution has opened up new avenues to study such challenging problems. Ironically the application of such models actually may result in an enhanced desire for detailed observations (at least in some limited geographical regions) for model evaluation. In this kind of approach, detailed diagnostics are computed from the complete model global fields and the model itself is validated against some specialized set of fine resolution observations. A recent project on tidal variations in the atmosphere has brought together such fine-resolution global modeling and a local-scale observational campaign. The project has also brought together the expertise of scientists at JAMSTEC, NOAA and the IPRC.

On a local scale, the daily cycle of solar radiation induces variations in the effective surface heating over land and ocean, creating land-sea breezes, and over topographic slopes, mountain-valley breezes. These local circulations are roughly balanced between radiatively driven horizontal pressure gradients

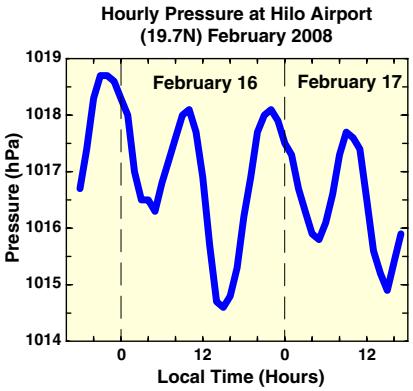

Figure 1. The hourly sea-level pressure for a typical 48-hour period at Hilo Airport (19.7°N, 155°W) plotted against local time. Data provided by the National Weather Service.

IPRC's Kevin Hamilton (right) and NOAA's Steve Ryan inspecting the pressure station located at the Mauna Loa Observatory.

and small-scale turbulent "friction"; they are generally restricted to the lowest 2–3 km of the atmosphere and have only small pressure signatures. On a larger horizontal scale, the pressure gradients caused by diurnal heating variations are balanced by Coriolis and acceleration terms, and the response can be regarded as large-scale inertia-gravity waves. On the global scale, this results in a large sun-following thermal tide that propagates vertically upward and/or downward from its forcing altitudes and is observed most readily from surface pressure measurements. This wave is conventionally resolved into diurnal (24 hour), semidiurnal (12 hour), terdiurnal (8 hour), etc. components. Although the tides contribute only modestly to barometric pressure variations in the extratropics, at low latitudes the daily tidal pressure variation, particularly that of the semidiurnal tide, exceeds that associated with typical day-to-day weather changes.

The amplitude and phase of the semidiurnal surface pressure oscillation, denoted S2(p), have now been determined at several hundred observation stations. The determinations are based on a simple Fourier analysis of long records of hourly barometric observations and are expressed as an amplitude and a local time phase (time of maximum). In the tropics and mid-latitudes, S2(p) is dominated by zonally-symmetric (in local time) components. The semidiurnal tide is excited most efficiently by coherent heating sources that extend over a deep layer of the atmosphere, notably by solar heating of the stratospheric ozone. Thus, to first order, the semidiurnal tide at the ground results from a global inertia-gravity wave propagating downward from the ozone layer. This wave (which looks zonally-symmetric when the phase is expressed in local time) interacts with orography at the earth's surface, leading to geographical modulations of S2(p).

An interesting implication of our theoretical understanding of the semidiurnal tide as a vertically-propagating wave is that the amplitude of the pressure perturbations by topography should vary roughly as the inverse square-root of the mean density. This suggests a first order effect of topography on S2(p) may simply be a reduction of amplitude over that at sea level at the same latitude. Earlier authors have noted that in several cases the S2(p) at high altitude stations appear to be anomalous relative to lower elevation stations, although this possibility apparently has not been explored systematically previously. There have been a number of earlier studies of the semidiurnal atmospheric tide that have used comprehensive global models dating back to the pioneering works of Zwiers and Hamilton (1986) and Tokioka and Yagai (1987). Since at that time those models had to be run at fairly coarse spatial resolution (horizontal grid spacing of 300 km or more), these studies could not adequately simulate the effects of regional topographic features.

IPRC Interim Director **Kevin Hamilton** and JAMSTEC's **Wataru Ohfuchi** (Leader of the Atmosphere and Ocean Simulation Research Group at the Earth Simulator Center) are collaborating to examine the S2(p) simulated in an ultra-high resolution version of the AFES (Atmospheric General Circulation Model for the Earth Simulator; Ohfuchi et al. 2004). Specifically, they are examining integrations with a version of the model with T1279 horizontal spectral resolution and 96 levels in the vertical up to about 60 km. The model spectral fields are reconstructed on a 3840x1920 latitude–longitude grid, corresponding roughly to a 10-km horizontal grid spacing. The model employs a slightly filtered version of realistic T1279 resolution topography. As an interesting aside, Hamilton has estimated that integrating the fine resolution AFES requires more than

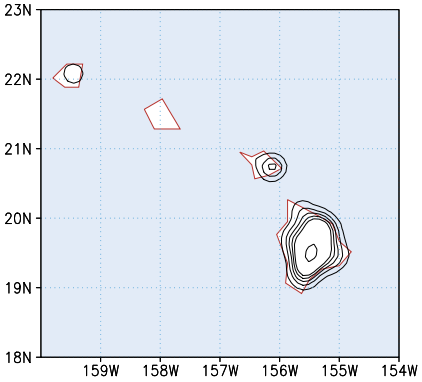

Figure 2. Topographic heights for the Hawaiian Islands as represented in the T1279 AFES model. Thin contours are for 200, 400, 600, 800 m, thick contours for 1000 and 2000 m.

one million times the computational effort per day of simulation as the models used by Tokioka and Yagai or Zwiers and Hamilton, which represented the state-of-the-art two decades ago! The amazing increase in computational power in the last two decades, including the advent of the JAMSTEC Earth Simulator in 2003, has opened entirely new avenues in atmospheric modelling.

In their analysis, Hamilton and Ohfuchi have found some small-scale features in the AFES-simulated semidiurnal surface-pressure tides in the vicinity of high and steep topography. While some limited observational support for these simulated patterns is available from previous single station determinations of S2(p) in various parts of the world, they identified a need for a set of observations of S2(p) concentrated around some large and steep topographic feature.

The Big Island of Hawai'i is an ideal test bed for the effects of tall and steep local topography on the tide. Hamilton and Ohfuchi have shown that in AFES the tall mountains of the island modulate the tides in interesting ways. Figure 2 shows the topography of the Hawaiian Islands as represented in the model. Due to the limited spectral resolution, it is unrealistically smooth, representing the Big Island as a single ridge oriented roughly north-south with a peak height of about

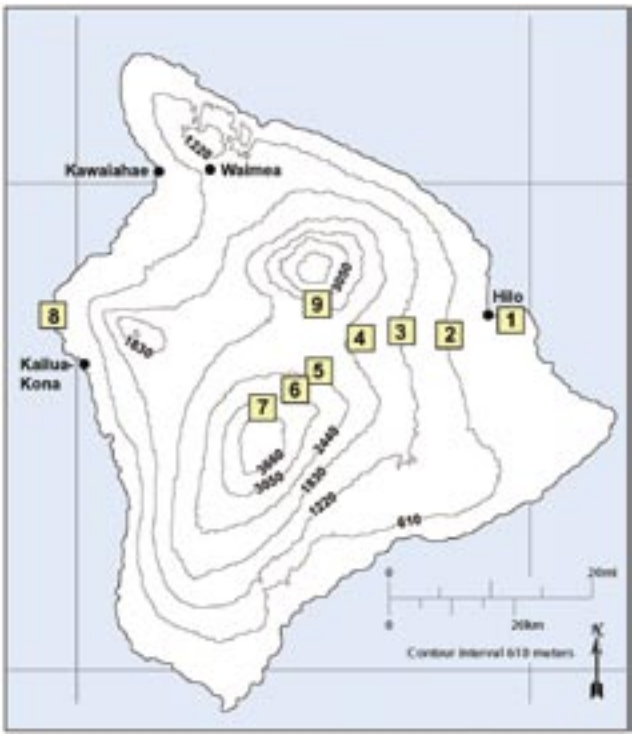

Figure 3. Topographic map of the Big Island of Hawai'i with the positions of the barometric stations deployed by the Mauna Loa Observatory marked as squares. Station numbers correspond to those in Figure 4.

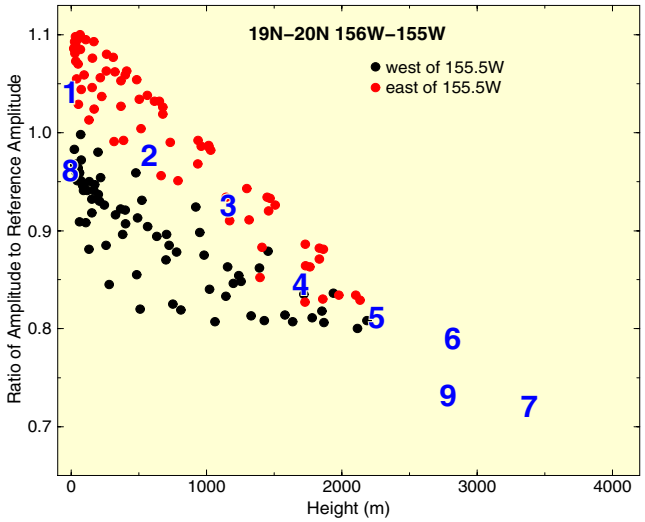

Figure 4. A plot of S2(p) amplitude and topographic height at individual grid points in the AFES simulation, where S2(p) amplitude at each grid point is divided by the average of the amplitudes at grid points near Hilo (east coast) and Kona (west coast; see text for details). Results are shown for the box 19°N–20°N, 155°W–156°W, with the eastern half in red and the western half in black. The blue numbers show the normalized two-year mean S2(p) amplitudes from barometric observations at the network of 9 stations shown in Figure 3. The observations are normalized by the average of the station amplitudes at Hilo and Kona.

2200 m. The island's real topography (shown in Figure 3) has two very tall peaks, Mauna Loa (4150 m) in the south and Mauna Kea (4200 m) in the north, separated by about 30 km and a valley dropping to about 2000 m. Despite the limitation in resolution, AFES should allow a reasonable topography-tide interaction for the region. In both the real world and the model topography, the distance between the highest points and sea level on the west coast of the island is roughly 50 km, resulting in quite steep mean slopes in the east-west direction (~.05–0.1). Each circle in Figure 4 shows the normalized S2(p) amplitude as simulated at one grid point and plotted as a function of the topographic elevation of the grid point in the model. The values are normalized by the amplitude means at the grid points closest to Hilo (model grid point at 19.72°N, 154.97°W) on the east coast and Kona (model grid point at 19.72°N, 156.0°W) on the west coast. Results are shown for points in the box 19°N–20°N, 155°W–156°W, which includes almost all the Big Island land mass and a small amount of surrounding ocean. Results for the eastern half of the box

are shown in red and for the western half in black, roughly corresponding to the grid points on the eastern and the western slopes. The general decay of pressure amplitude with height is very evident. The amplitudes, moreover, are clearly higher on the eastern than the western slopes.

Hamilton and Ohfuchi suggest a simple explanation for these results: the low S2(p) amplitudes on the west side are due to wave scattering by the mountains. Figure 5 shows a schematic of the group velocity associated with a large-scale inertia-gravity wave directed downward and westward towards a topographic feature. Simple-plane wave theory for a wave with semidiurnal frequency would predict a slope of 0.015 from the horizontal for the group velocity vector. It is reasonable to expect that steep topography casts a long "shadow" to the west, reducing the S2(p) amplitude in the shadow region.

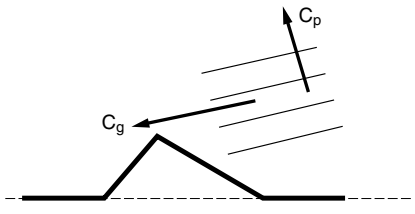

Figure 5. A schematic of a large-scale inertia-gravity wave directed downwards and westward towards a topographic feature.

In a quest for observational support of their model results, Hamilton and Ohfuchi have teamed up with **Steve Ryan** of the NOAA Mauna Loa Observatory (MLO). MLO has deployed a network of 9 identical data-logging instruments recording surface pressure and surface air temperature at 1 second intervals across the Big Island. The station locations are shown in Figure 3. Station #1 is at Hilo Airport and station #8 is at Kona Airport. Station #7 is at elevation 3396 m at the Mauna Loa Observatory on the north slope of Mauna Loa, almost due north from the summit. Stations #2 to 6 lie in a rough line between Hilo and MLO ascending the northeast slope of Mauna Loa, and station #9 is on the south slope of Mauna Kea at 2797 m, almost due south of the summit. The network allows an unprecedented sampling of S2(p) over a large range of elevations in a small geographical region.

S2(p) amplitude and phase for the station network have been determined from two full years of observations. The amplitude for each station, normalized by the mean of the values at Kona and Hilo, is plotted as a function of elevation in Figure 4 for easy comparison with the AFES grid point results. A tendency for amplitude to drop off with height is apparent in the station observations, and the rate of decrease with height is comparable to that in the AFES simulation. Also the contrast in amplitude between Hilo and Kona provides some observational support for the east-west asymmetry of S2(p) across the Big Island in the AFES simulation. Specifically, the ratio of the observed S2(p) amplitude at Hilo to that at Kona is 1.08; the AFES simulated amplitudes at the grid points near Hilo and Kona are also in the ratio of 1.08. The simulated local time phases of S2(p) are 9.44 hours at the grid point near Hilo and 9.64 hours at the grid point near Kona, showing a similar contrast as the observed station values (9.50 and 9.60).

This study used the AFES simulations to investigate longstanding issues in the regional modulation of the semidiurnal tide. Numerical weather prediction models are being run in major operational centers at increasingly fine spatial resolution. A realistic simulation of the topographic modulation of the daily pressure variation in such models should help to accurately assimilate surface pressure observations, and thus improve weather predictions. The study also provided a chance to evaluate the AFES model itself. It is encouraging that this high-resolution model is able to successfully simulate such detailed regional structures as found in S2(p).

References

Ohfuchi, W., and coauthors, 2004: 10-km mesh meso-scale resolving simulations of the global atmosphere on the Earth Simulator -Preliminary outcomes of AFES. *J. Earth Simulator*, **1**, 8–34.

Tokioka, T., and I. Yagai, 1987: Atmospheric tides appearing in a global atmospheric general circulation model. *J. Meteor. Soc. Japan*, **65**, 423–438.

Zwiers, F. and Hamilton, K., 1986. Simulation of solar tides in the Canadian Climate Centre general circulation model. *J. Geophys. Res.*, **91**, 11,877–11,896.

iprc